# Theoretical Study of the Low Lying Electronic States of oxoX(salen) (X = Mn, $Mn^-$, Fe, and $Cr^-$) Complexes

**Joseph Ivanic,* Jack R. Collins, and Stanley K. Burt**

*Advanced Biomedical Computing Center, National Cancer Institute at Frederick, Contract No. N01-CO-12400, SAIC Frederick, P.O. Box B, Frederick, Maryland 21702-1201*

*Received: October 31, 2003; In Final Form: January 16, 2004*

The lowest lying electronic states of oxoX(salen) (X = Mn, Mn-, Fe and Cr) complexes have been studied using complete active space self-consistent field (CASSCF) calculations. These wave functions have been analyzed, via the use of localized and natural orbitals, to identify the electronic structure contributions to the chemistry of these systems. It is found that the electronic structures of all complexes can be rationalized through the use of a common orbital energy diagram. Single point multireference Moller−Plesset (MRMP2) perturbation theory calculations have been performed for the oxoMn(salen) system and these results verify that the CASSCF method gives accurate energy separations for the electronic states. We find that the CASSCF method predicts bound species for all compounds except for the triplet and quintet states of the oxoMn-(salen) complex, which spontaneously dissociate in the gas phase. Calculations on the separated species [$^5$A Mn(salen) + $^3$P O] indicate that the bound singlet species lies some 30 kcal/mol above the dissociated products at the CASSCF level. Attempts to obtain MRMP2 energies for the supersystem of the separated species failed; hence a more accurate value of the dissociation energy could not be determined. We also find, from CASSCF calculations, that the oxoMn(salen) complex is predicted to be a very potent electrophile.

## 1. Introduction

Over the past decade, several techniques that control the product specificity during asymmetric epoxidation of unfunctionalized olefins have been developed[1] and have become very important in organic synthesis strategies. Of these, the Jacobsen−Katsuki epoxidation is one of the most important because high enantiomeric excesses and yields can be achieved,[2] and the Mn(salen) catalyst used in these reactions has become one of the most important in this field. This remarkable selectivity has led to many experimental studies aimed at understanding the mechanistic steps in the reaction and the properties that modulate the specificity. Individual results, however, have lent support for one of three different reaction mechanisms: concerted,[3] stepwise radical,[4] and metallooxetane mediated.[5] The dilemma of how best to interpret these observations becomes further complicated by more recent experimental data ,which suggest that the electronic properties of the ligand substituents of the Mn(salen) catalyst directly influence the ratio of isomers in the product.[6] In addition to their synthetic applications, Mn-(salen) compounds have also been designed as therapeutic agents to mimic the activity of superoxide dismutase and catalase for the destruction of radical oxygen species.[7] To address these questions, several theoretical studies were performed on oxoMn-(salen) models.

Linde et al. used hybrid density functional theory (DFT/B3LYP) to study the reaction of the simplified cationic model without the chlorine ligand,[8] illustrated in Figure 1. The singlet, triplet, and quintet states were studied and found to be nearly degenerate, with only 2.6 kcal/mol separating all three spin states. They predicted that the reaction initially proceeds upon a triplet surface and then spin flips such that a quintet surface is finally followed. The singlet pathway was predicted to be energetically uncompetitive because formation of the products was found to be endothermic. Jacobsen et al. also used the DFT method but with a different functional (CGA-BP86) to study the reaction of the chlorine containing neutral model[9] illustrated in Figure 1. They also predicted that a triplet surface is initially followed but saw no evidence of a jump to a quintet surface; i.e., it was concluded that the triplet spin of the system is conserved during the reaction. A more recent DFT study employing the BP86 functional, also using the neutral model system, found that the singlet state of the Mn(salen)oxo system was the most stable followed by the triplet and quintet states at 6.7 and 17.6 kcal/mol, respectively. This study also performed CCSD(T) calculations for comparison and found qualitatively similar results. They concluded that the singlet pathway is competitive with the triplet and suggest, on the basis of DFT and CCSD(T) calculations, that this was the most likely channel.[10] These discrepancies lead to qualitatively different

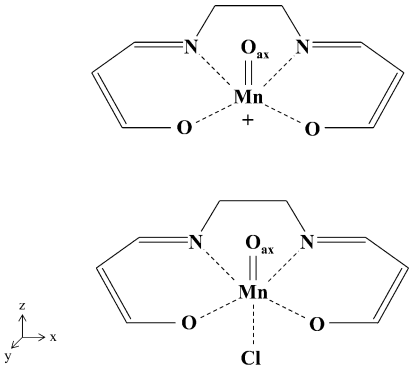


**Figure 1.** Illustrations of the cationic and neutral models of the (salen)-Mn catalysts used in the theoretical studies.

* Corresponding author. Phone: (301) 846-5550. Fax: (301) 846-5762. E-mail: jivanic@ncifcrf.gov.

10.1021/jp031214g CCC: $27.50 
Published on Web 02/27/2004

pictures of the oxoMn(salen) complex and subsequent reactions with olefins.

The previous DFT calculations used different functionals (BP86 vs B3LYP) and have come to qualitatively different conclusions concerning these systems, primarily due to the electronic description of the excited states and their multiconfigurational nature. None of the previous calculations have presented a detailed picture of the electronic configurations leading to the singlet, triplet, and quintet spin states that are central to understanding the reaction and lie at the heart of the discrepancies. To address these issues, we present here a complete active space self-consistent field (CASSCF) study of this neutral system, illustrated in Figure 1.[11] All three spin states are studied and the nature of their electronic structures are obtained through generation of localized orbitals and natural orbitals(NOs). Single point multireference Moller−Plesset (MRMP2) peturbation theory calculations have been performed to get better estimates of the relative energies. We have also performed CASSCF calculations on related species in which the central Mn metal is replaced by $Mn^-$, Fe, and $Cr^-$ so that their electronic structures and orderings of spin states may be better understood in relationship to the role of the metal in modulating the electronic structure. The results of our calculations present a consistent picture of the electronic structure of these systems and, through investigation of natural orbitals (NOs), clearly show the multiconfigurational behavior of the wave functions.

## 2. Methodology

Two basis sets were used in this study. The first of these is the 6-31G*[12] set. This set is more commonly labeled 6-31G(d) for elements up to Ar, and 6-31G* for elements K−Zn. This basis was used for all systems and in each case yielded a total of 273 Cartesian functions. The second basis set basis consists of the 6-31G(d) set for all atoms except Cl and Mn, for which the SBKJC VDZ ECP sets[13] were used. The Cl and Mn sets were augmented with single d and f polarization functions, respectively. The exponents of these polarization functions are $\alpha_d(Cl) = 0.75$ and $\alpha_f(Mn) = 0.8$. This basis set, hereafter labeled ECP, also yielded a total of 273 Cartesian functions and was used for the Mn(salen) and $Mn(salen)^-$ systems.

All calculations were executed using the GAMESS package.[14] Geometry optimization at the SCF level was performed only for the singlet and triplet states of the Mn(salen) complex to generate starting orbitals for CASSCF calculations. Geometry optimizations at the CASSCF level of theory were performed for all complexes. Descriptions of the CASSCF active spaces and generation of initial guess orbitals are given below. CASSCF calculations were executed using a previously described determinant FCI code[15] coupled with two orbital optimization methods. Calculations with the 6-31G* basis set used the approximate second-order orbital optimization method of Chaban, Schmidt, and Gordon.[16] When the ECP basis set was used, this method failed to converge in most cases and in these instances the second-order orbital optimization program of Dupuis[17] and its parallel implementation[18] were used. For the oxoMn(salen) systems, single point MRMP2[19] energies were obtained using the MCQDPT2 program of Nakano.[20] Localizations of orbitals (SCF and CASSCF) were executed using the Edmiston−Ruedenberg[21] procedure and orbital illustrations were prepared using the WinMolPlt program of Olson et al.[22]

## 3. Results

The four systems, oxoMn(salen), $oxoMn(salen)^-$, oxoFe(salen), and $oxoCr(salen)^-$, were studied in the order given. All of these complexes contain no symmetry elements, and therefore all calculations were performed in $C_1$ symmetry. For the oxoMn(salen) and $oxoCr(salen)^-$ complexes, singlet, triplet, and quintet states were studied. For the $oxoMn(salen)^-$ and oxoFe(salen) species, doublet and quartet states were studied. Generation and description of the CASSCF active spaces for the oxoMn(salen) complex is given in the next section. These active orbitals remain qualitatively equivalent for all species with geometries containing close metal−$O_{ax}$ distances, only the occupation numbers are seen to change. For the oxoMn(salen) complex, dissociated products Mn(salen) + O were also studied for reasons described below.

**A. oxoMn(salen).** *I. Singlet.* SCF Orbitals. Geometry optimization was performed at the RHF/6-31G* level. There is a total of 69 doubly occupied orbitals. The resulting structure together with the two highest occupied canonical molecular orbitals (HOMOs) and two lowest unoccupied canonical molecular orbitals (LUMOs) are given in Figure 2. We see that the RHF/6-31G* optimized geometry has a pseudooctahdral structure with the Mn atom residing slightly above the basal ligand plane. The two HOMOs are very similar and consist of contributions from a number of areas, the largest being the alkene $\pi$ orbitals on each ring and Cl orbitals. The LUMOs clearly represent Mn−$O_{ax}$ antibonding $\pi^*$ orbitals. The occupied RHF orbitals were localized to ascertain the "chemistry" occurring in the system. We find the expected $\sigma$ bonds occurring in the salen ligand and also four Cl sp hybridized valence orbitals, indicating that the Cl atom is essentially a $Cl^-$ anion. We also find three $\pi$-type orbitals on each ring, indicating that each side of the ligand has acquired an extra electron from the Mn center. Of these six salen $\pi$ orbitals, two represent C−N $\pi$ bonds, two represent C−O $\pi$ bonds, and the remaining two represent C−C−C type $\pi$ orbitals. These last two, labeled hereafter as R$\pi$1 and R$\pi$2, contribute significantly to the two canonical HOMOs and are illustrated in Figure 3. Additionally, we find that each of the N and O atoms in the ligand have a lone pair involved in dative bonding with a d orbital of the Mn atom and these are also illustrated in Figure 3. Each salen O has an additional lone-pair orbital not involved in any bonding interactions. Finally we obtained three Mn−$O_{ax}$ bonds, an $O_{ax}$ lone pair and a Mn d lone pair. The Mn−$O_{ax}$ bonding and Mn d lone-pair orbitals will be discussed in more detail below as part of the CASSCF active space. It is important to note that all five d orbitals in the Mn system have been accounted for and that one of these is doubly occupied for the singlet case.

CASSCF Wave Functions. We initially tried to perform a CASSCF/6-31G* calculation with an active space consisting of 12 electrons in 11 orbitals and 63 core orbitals. The active orbital set consisted of the six SCF occupied orbitals d[$x^2-y^2$](Mn), R$\pi$1, R$\pi$2, $\sigma$(Mn$O_{ax}$), $\pi$1(Mn$O_{ax}$), and $\pi$2(Mn$O_{ax}$) together with the correlating orbitals R$\pi$1*, R$\pi$2*, $\sigma^*$(Mn$O_{ax}$), $\pi$1*(Mn$O_{ax}$), and $\pi$2*(Mn$O_{ax}$). Here d[$x^2-y^2$](Mn) refers to the doubly occupied d lone pair, R$\pi$1 and R$\pi$2 refer to the C−C−C type $\pi$ orbitals, and $\sigma$(Mn$O_{ax}$), $\pi$1(Mn$O_{ax}$), and $\pi$2(Mn$O_{ax}$) refer to the $\sigma$ and two $\pi$ Mn−$O_{ax}$ bonding orbitals. The initial guess correlating orbitals were obtained by generation of modified virtual orbitals (MVOs).[23] During the CASSCF optimization, however, the active d[$x^2-y^2$](Mn) orbital switched with a Cl valence orbital in the core space. This should not have been such a surprise as there was not a correlating orbital for the d(Mn) lone pair present in the active space. This d[$x^2-y^2$](Mn) orbital was subsequently constrained to be doubly occupied in all configurations, i.e., moved into the core space, and the CASSCF optimization for the 10 electron, 10 orbital active space

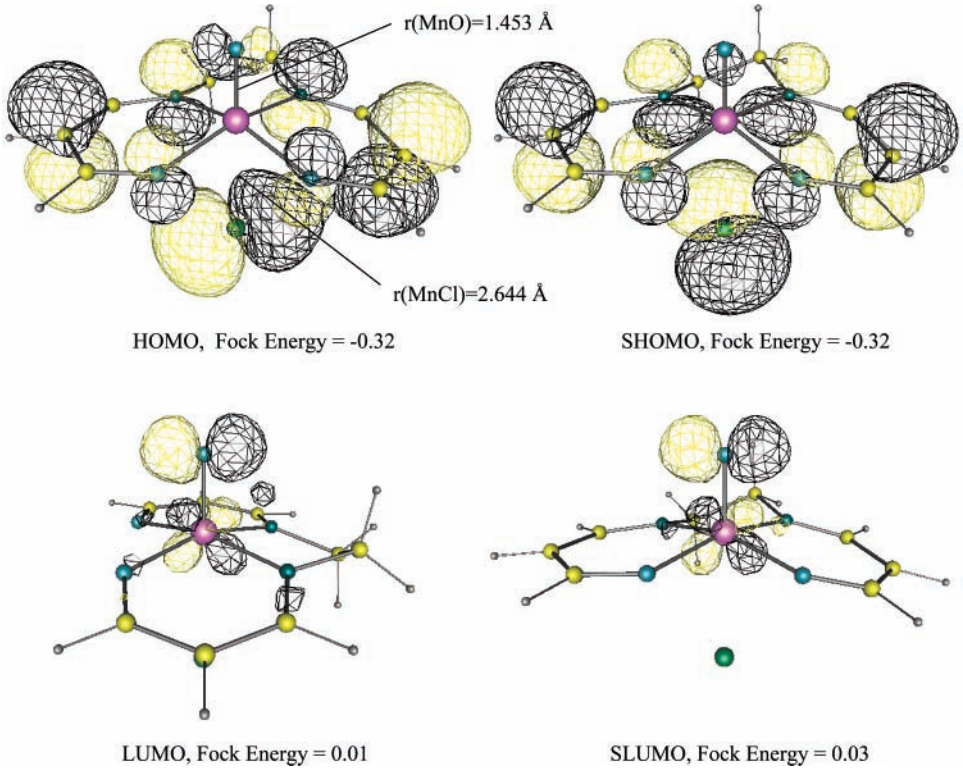


**Figure 2.** oxoMn(salen) RHF/6-31G* optimized geometry together with illustrations of the two highest occupied canonical molecular orbitals and the two lowest unoccupied canonical molecular orbitals. Fock energies, in hartrees, are given below each orbital.

converged with little trouble. For this active space there was a total of 64 504 determinants with $M_s = 0$ in the configuration space. The singlet geometry was optimized at this level of theory, NOs were generated and the core orbitals localized. The CASSCF absolute energy is given in Table 1. Figure 4 shows the optimized geometry, the ten NOs together with their occupation, and the d[$x^2-y^2$](Mn) localized orbital. One immediately notices that the Mn−$O_{ax}$ distance has increased from the RHF value of 1.453 to 1.540 Å and the Mn−Cl distance has decreased from 2.664 to 2.468 Å. The structure has become more octahedral in going from RHF to the CASSCF level of theory with the Mn atom now residing within the basal ligand plane. The NOs clearly resemble the intended active space described above in that the antibonding correlating orbitals have been determined properly. It is also clear that there are three Mn−$O_{ax}$ bonding orbitals and that excitations into their antibonding counterparts are not insignificant. We also note the presence of the d[$x^2-y^2$](Mn) lone pair, which will prove vital for the description of the higher spin states. Figure 5 illustrates the electronic structure of the singlet.

A CASSCF study with the ECP basis set yielded essentially equivalent results to that described above for the 6-31G* basis. The optimized geometry has an Mn−$O_{ax}$ bond length of 1.541 Å, 0.001 longer than that obtained with the 6-31G* basis. The absolute energy for the optimized singlet species is given in Table 1. NOs obtained when the two basis sets are used are qualitatively equivalent and localized core orbitals for the ECP basis set confirm the existence of a d[$x^2-y^2$](Mn) lone pair.

MRMP2 Energies. MRMP2 energies at the CASSCF optimized geometries for both basis sets were obtained for an orbital space containing 27 frozen core orbitals, 36 valence doubly occupied orbitals and a 12 electron, 11 orbital FCI space. All virtual orbitals were allowed to be occupied. All orbitals were taken from the CASSCF wave functions described above. The FCI active space consisted of the 10 active CASSCF orbitals together with the localized d[$x^2-y^2$](Mn) lone pair. Absolute energies are given in Table 1.

*II. Triplet.* SCF Orbitals. Starting from an open shell triplet SCF orbital optimization using the closed shell orbitals as initial guess results in a R$\pi \rightarrow \pi^*$(Mn$O_{ax}$) excitation as the initial description of the triplet state. This suggests that an electron jumps from a ring $\pi$ orbital and into a Mn−$O_{ax}$ antibonding $\pi$ orbital. This is essentially an electron transfer where an electron has migrated from the ligand to the center of the molecule. Optimization of this triplet state leads to a structure that has the axial oxygen atom shifted sideways toward one of the rings. We were puzzled by this single determinant description of the next highest triplet state was so CASSCF calculations, described immediately below, were performed.

CASSCF Wave Functions. After validating that we had a correct CASSCF electronic description of the singlet, we proceeded to a study of the triplet state. The active space described above for the singlet was used as a starting point for the triplet CASSCF/6-31G* study, except for one difference, the d[$x^2-y^2$](Mn) lone pair was also included in the active space. The initial FCI for these orbitals, constituting 152 460 determinants with $M_s = 1$, clearly showed that the two lowest triplet states were the result of a single electron excitation from the d[$x^2-y^2$](Mn) lone pair orbital into the $\pi 1^*$(Mn$O_{ax}$) and $\pi 2^*$-(Mn$O_{ax}$) orbitals. These two triplet states are very close in energy but not degenerate due to the $C_1$ symmetry of the system. This multiconfigurational result is in stark disagreement with the SCF description. CASSCF optimization of the lowest triplet state at the singlet geometry yielded NOs almost indistinguishable from those obtained for the singlet, with the only difference being that the $\pi 1$(Mn$O_{ax}$), $\pi 2$(Mn$O_{ax}$), $\pi 1^*$(Mn$O_{ax}$), and $\pi 2^*$-(Mn$O_{ax}$) orbitals have been rotated clockwise about the Mn−$O_{ax}$ axis by approximately 20° when one looks down from $O_{ax}$ to Mn. NO occupations for the R$\pi 1$, R$\pi 1^*$, R$\pi 2$, R$\pi 2^*$,

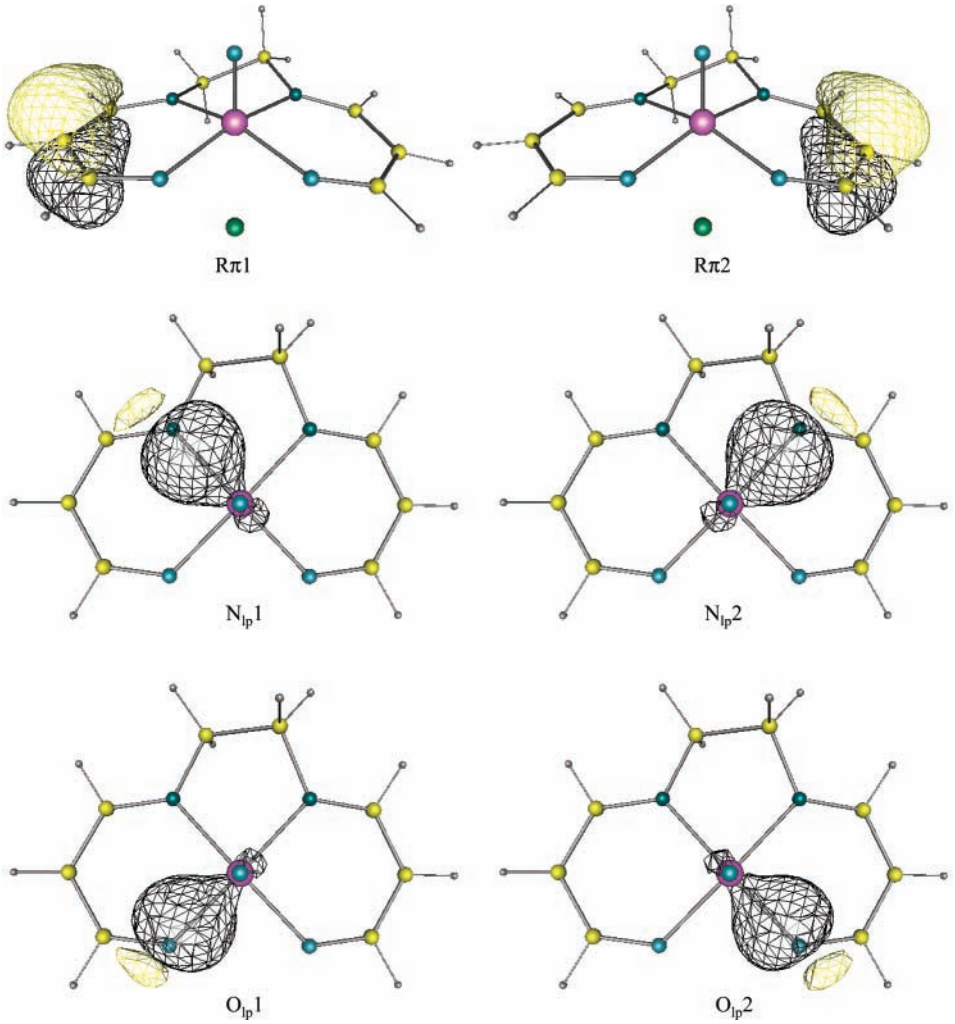


**Figure 3.** Illustrations of the six localized RHF/6-31G* orbitals for the oxoMn(salen) complex. Shown are the two C−C−C ring $\pi$ orbitals and the four N, O lone pairs interacting with the central Mn atom.

**TABLE 1: Absolute Energies (hartrees) of the Systems Studied in This Work**

| system | CASSCF/6-31G* | CASSCF/ECP | MRMP2/6-31G*[a] | MRMP2/ECP[a] |
|---|---|---|---|---|
| $^1$A oxoMn(salen) | −2251.42550 | −760.09743 | −2253.60245 | −762.29597 |
| $^3$A oxoMn(salen)[a] | −2251.43011 | −760.10182 | −2253.60615 | −762.29779 |
| $^5$A oxoMn(salen)[a] | −2251.36220 | −760.03446 | −2253.53069 | −762.22169 |
| $^5$A Mn(salen) | −2176.69981 | −685.37211 | | |
| $^3$P O | −74.77897 | −74.77897 | | |
| $^2$A oxoMn(salen)$^-$ | −2251.52938 | −760.19825 | | |
| $^4$A oxoMn(salen)$^-$ | −2251.54425 | −760.21357 | | |
| $^2$A oxoFe(salen) | −2363.98483 | | | |
| $^4$A oxoFe(salen) | −2363.98002 | | | |
| $^1$A oxoCr(salen)$^-$ | −2145.19106 | | | |
| $^3$A oxoCr(salen)$^-$ | −2145.18945 | | | |
| $^5$A oxoCr(salen)$^-$ | −2145.14274 | | | |

[a] Reported energies are for the $^1$A oxoMn(salen) CASSCF optimized geometries because the triplet and quintet optimizations resulted in spontaneous dissociation of the axial oxygen atom.

$\sigma$(MnO$_{ax}$), and $\sigma$*(MnO$_{ax}$) orbitals are similar to their singlet counterparts at 1.97, 0.03, 1.96, 0.05, 1.88, and 0.12, respectively. Occupations for the remaining $\pi$1(MnO$_{ax}$), $\pi$1*(MnO$_{ax}$), $\pi$2(MnO$_{ax}$), $\pi$2*(MnO$_{ax}$), and d[$x^2-y^2$](Mn) orbitals are 1.68, 0.33, 1.95, 1.05, and 1.00, respectively. These are, as expected, different from the singlet species and indicate that the lowest triplet state has the dominant d$^1\pi^{*1}$ configuration. Figure 5 illustrates the excitation from the singlet configuration which gives rise to the triplet. The absolute CASSCF energy is given in Table 1 and the relative energy with respect to the singlet is given in Table 2. One sees that the triplet at the singlet geometry is predicted to lie 2.9 kcal/mol lower than the singlet for this level of theory. Even though the d[$x^2-y^2$](Mn) lone pair orbital is not included in the singlet active space, we feel that the two energies are comparable as the d[$x^2-y^2$](Mn) orbital did not have a correlating orbital in either case and preferred to be doubly occupied in all configurations for the singlet wave function. Geometry optimization of the triplet at this CASSCF/6-31G* level of theory spontaneously dissociated the O atom. Starting the geometry optimization with a longer Mn−O$_{ax}$ distance of 1.72 Å and the same active space led to the same result.

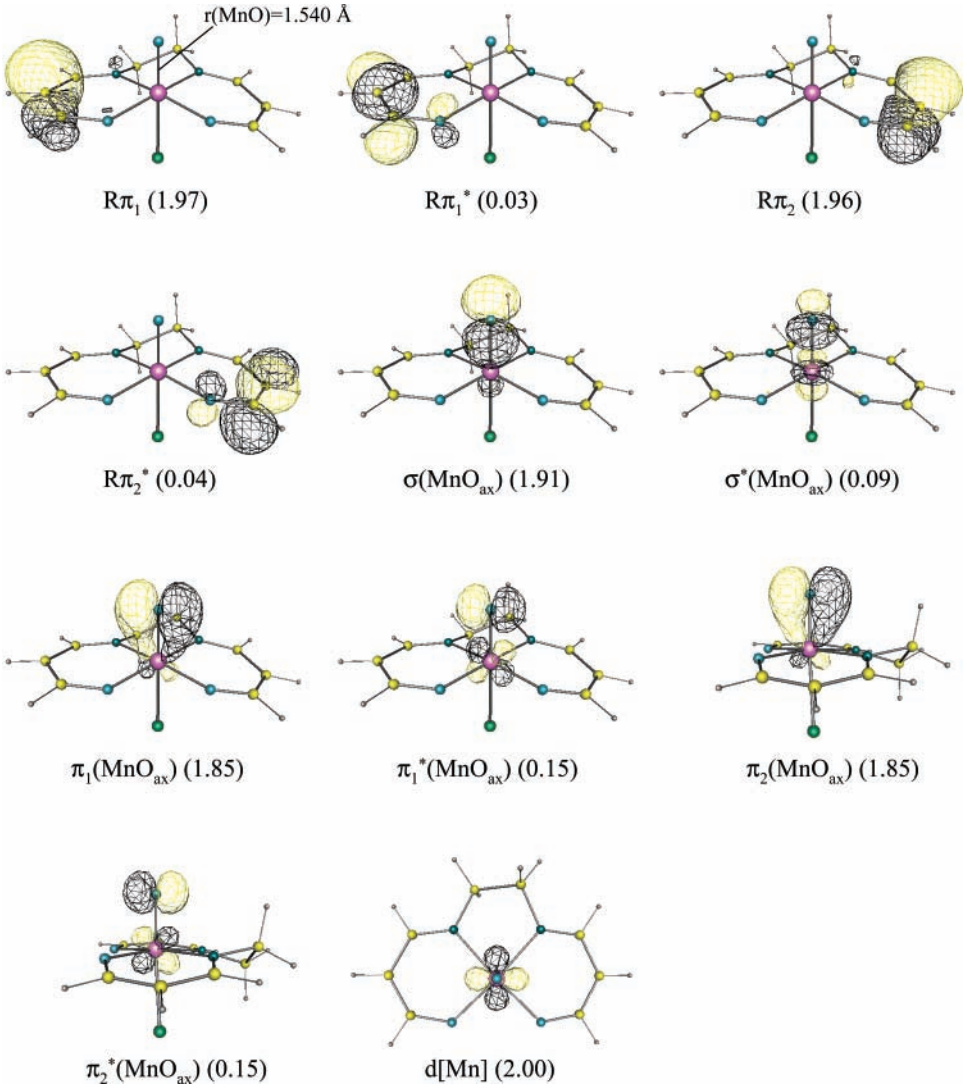


**Figure 4.** oxoMn(salen) CASSCF/6-31G* optimized geometry together with plots of the 10 natural orbitals and the d[$x^2-y^2$](Mn) localized core orbital. Occupations are given below each illustrations.

**TABLE 2: Relative Energies (kcal/mol) of the Systems Studied in This Work**[a]

| system | CASSCF/6-31G* | CASSCF/ECP | MRMP2/6-31G*[b] | MRMP2/ECP[b] |
|---|---|---|---|---|
| $^1$A oxoMn(salen) | 0 | 0 | 0 | 0 |
| $^3$A oxoMn(salen)[b] | −2.9 | −2.8 | −2.3 | −1.1 |
| $^5$A oxoMn(salen)[b] | 39.7 | 39.5 | 45.0 | 46.6 |
| $^5$A Mn(salen) + $^3$P O[c] | −33.4 | −33.7 | | |
| $^2$A oxoMn(salen)$^-$ | 0 | 0 | | |
| $^4$A oxoMn(salen)$^-$ | −9.3 | −9.6 | | |
| $^2$A oxoFe(salen) | 0 | | | |
| $^4$A oxoFe(salen) | 3.0 | | | |
| $^1$A oxoCr(salen)$^-$ | 0 | | | |
| $^3$A oxoCr(salen)$^-$ | 1.0 | | | |
| $^5$A oxoCr(salen)$^-$ | 30.3 | | | |

[a] Energies are relative to the lowest spin state of the comparable species. [b] Calculations performed at $^1$A oxoMn(salen) CASSCF optimized geometries. [c] Energy is calculated relative to $^1$A oxoMn(salen) species.

This unexpected dissociation led us to perform a CASSCF study using the ECP basis set. As for the singlet case, optimized CASSCF NOs were qualitatively equivalent for the 6-31G* and ECP basis sets. The absolute CASSCF/ECP energy at the singlet optimized geometry is given in Table 1 and the relative energy with respect to the singlet is given in Table 2. We find that the triplet is predicted to lie lower than the singlet by 2.8 kcal/mol, almost exactly the same as that found using the 6-31G* basis. Again, full geometry optimization led to spontaneous dissociation of the O atom.

MRMP2 Energies. MRMP2 triplet energies at the CASSCF optimized singlet geometries for the two basis sets were determined using exactly the same orbital space dimensions as described for the singlet, the only difference being that triplet CASSCF optimized orbitals were used. Absolute energies are given in Table 1, and energies relative to the singlet MRMP2 energies are given in Table 2. We find that at this level of theory the triplet is predicted to lie lower than the singlet by 2.3 and 1.1 kcal/mol for the 6-31G* and ECP basis sets, respectively. These numbers are in good agreement with relative energies

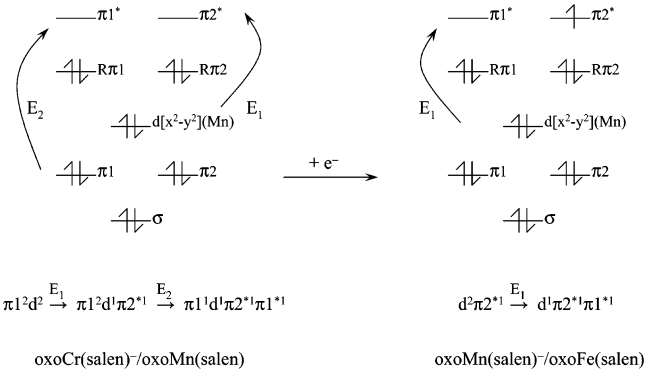


**Figure 5.** Illustrations of electronic structures of low spin oxo−transition-metal(salen) complexes and the electron excitations responsible for the higher spin states. Below these are configurations containing the important orbitals and their occupations which qualitatively describe the states. The $\sigma$, $\pi 2$, R$\pi 1$, and R$\pi 2$ orbitals are essentially doubly occupied in all cases.

obtained from CASSCF calculations. Consistent results are obtained for both basis sets and levels of theory.

*III. Quintet.* CASSCF Wave Functions. The active spaces described above for the triplet were used as a starting point for CASSCF studies of the quintet. The intial FCI, constituting 54 450 determinants with $M_s = 2$, for both basis sets predicted that the two lowest quintet states were a result of single electron excitation from the $\pi 1(MnO_{ax})$ or $\pi 2(MnO_{ax})$ orbitals into the $\pi 1^*(MnO_{ax})$ orbital. These two quintets are very close in energy but not degenerate due to the $C_1$ symmetry of the system. CASSCF optimization of the lowest quintet state gave NOs almost identical to those obtained for the triplet with the difference that the $\pi 1(MnO_{ax})$, $\pi 2(MnO_{ax})$, $\pi 1^*(MnO_{ax})$, and $\pi 2^*(MnO_{ax})$ orbitals have been rotated counterclockwise about the Mn−$O_{ax}$ axis by approximately 45° when one looks down from $O_{ax}$ to Mn. For the 6-31G* basis set, NO occupations for the R$\pi 1$, R$\pi 1^*$, R$\pi 2$, R$\pi 2^*$, $\sigma(MnO_{ax})$, and $\sigma^*(MnO_{ax})$ orbitals are similar to their singlet and triplet counterparts at 1.96, 0.04, 1.96, 0.04, 1.90, and 0.10, respectively. Occupations for the remaining $\pi 1(MnO_{ax})$, $\pi 1^*(MnO_{ax})$, $\pi 2(MnO_{ax})$, $\pi 2^*(MnO_{ax})$, and d[$x^2-y^2$](Mn) orbitals are 1.00, 1.00, 1.97, 1.03, and 1.00, respectively. This indicates that the lowest quintet has the dominant $d^1\pi 1\pi 1^{*1}\pi 2^{*1}$ configuration. Figure 5 illustrates the excitation from the triplet configuration which gives rise to the quintet. NOs and their occupations were qualitatively the same for both 6-31G* and ECP basis sets. Absolute energies are given in Table 1 and relative energies with respect to the singlet are given in Table 2. We see that the quintet species is predicted to be higher in energy than both singlet and triplet species, at the singlet optimized geometries, with predicted singlet-quintet gaps of 40 kcal/mol. As with the triplet case, geometry optimization led to spontaneous dissociation of the $O_{ax}$ atom when both basis sets were used.

MRMP2 Energies. MRMP2 quintet energies at the singlet geometries were obtained using the same orbital space dimensions as described for the triplet except that quintet CASSCF optimized orbitals were used. Absolute energies are given in Table 1, and energies relative to the singlet MRMP2 energies are given in Table 2. We find that at this level of theory the quintet is predicted to be higher than the singlet by 45 and 47 kcal/mol when the 6-31G* and ECP basis sets are used, respectively. We again find that relative energies predicted by both CASSCF and MRMP2 levels of theory are in reasonable agreement when the 6-31G* and ECP basis sets are used.

*IV. Dissociated Products:* $^5$*A Mn(salen)* + $^3$*P O.* The predicted spontaneous dissociation of the $O_{ax}$ atom for the triplet and quintet states, at the CASSCF level of theory, led us to investigate the stability of the oxoMn(salen) species relative to its dissociated products. We are reasonably sure, from preliminary calculations,[24] that the quintet is the lowest electronic state of the Mn(salen) species and this is in line with previous theoretical studies.[9a] The active spaces described above for the triplet and quintet states are such that they can correctly describe the separated products: $^5$A Mn(salen) + $^3$P O. This being the case, we performed separate CASSCF calculations on the quintet Mn(salen) and triplet O systems knowing that we can directly compare their combined energies with that of the oxoMn(salen) species.

CASSCF Wave Functions. It is well-known that the ground state for O is the $^3$P state. Its absolute CASSCF/6-31G(d) energy, which had all three p orbitals active, is given in Table 1. We note that both of the 6-31G* and ECP basis sets described above contain the 6-31G(d) set on $O_{ax}$. For the quintet Mn(salen) complex, an ROHF calculation adequately determined the four d[Mn] orbitals required for the CASSCF active space. Initial guess R$\pi 1^*$ and R$\pi 2^*$ orbitals were not obtained using the MVO method as the presence of four singly occupied d[Mn] orbitals in the ROHF determinant introduced difficulties. These were instead determined by performing a CISD calculation in which only the R$\pi 1$ and R$\pi 2$ orbitals were allowed to be excited out of and into the lowest ninety canonical virtual orbitals. NOs for this wave function provided good initial guesses for the R$\pi 1^*$ and R$\pi 2^*$ orbitals. An active space constituting the R$\pi 1$, R$\pi 2$, R$\pi 1^*$, R$\pi 2^*$, and four d[Mn] orbitals was used for the quintet calculations. CASSCF wave functions for this 8 orbital, 8 electron space, containing 784 determinants with $M_s = 2$, converged without difficulty for both basis sets and geometries were subsequently optimized at this level of theory. Table 1 gives absolute energies for the quintet Mn(salen) system. Figure 6 illustrates the CASSCF/6-31G* optimized geometry together with the NOs and their occupation numbers. We see that the Mn atom has moved slightly below the basal ligand plane to produce a structure that is more square pyramidal than the oxoMn(salen) geometry. The environment around the Mn atom is very similar to that observed for the experimental structure of the related $C_{36}H_{52}N_2O_2ClMn$ species.[25] The R$\pi 1$, R$\pi 2$, R$\pi 1^*$, and R$\pi 2^*$ orbitals and their occupations are essentially equivalent to their counterparts in the oxoMn(salen) species. We also observe the classical picture of four d(Mn) singly occupied orbitals. Geometries and NOs obtained using the ECP basis set are qualitatively equivalent to those obtained using the 6-31G* basis.

*V. Stability of oxoMn(salen) Species.* Total energies for the dissociated species were obtained by simply adding together the energies obtained for the quintet Mn(salen) species to the energy obtained for the triplet O atom. The energies of the separated system relative to that of the singlet oxoMn(salen) species is given in Table 2. We find that the dissociated system is predicted to lie lower than the singlet oxoMn(salen) species by 33 and 34 kcal/mol at the CASSCF/6-31G* and CASSCF/ECP levels of theory, respectively. Thus the triplet species, at the singlet optimized geometry, lies some 30 kcal/mol above the separated products and the quintet species, at the singlet geometry, lies a further 40 kcal/mol higher. These large dissociation energies are consistent with there being no observation of any barriers for the dissociations of the triplet and quintet species in our calculations. However, the singlet species is observed to have a bound minimum, despite its large apparent instability. It can be shown using simple spin arguments that the singlet species cannot dissociate into the quintet Mn(salen)

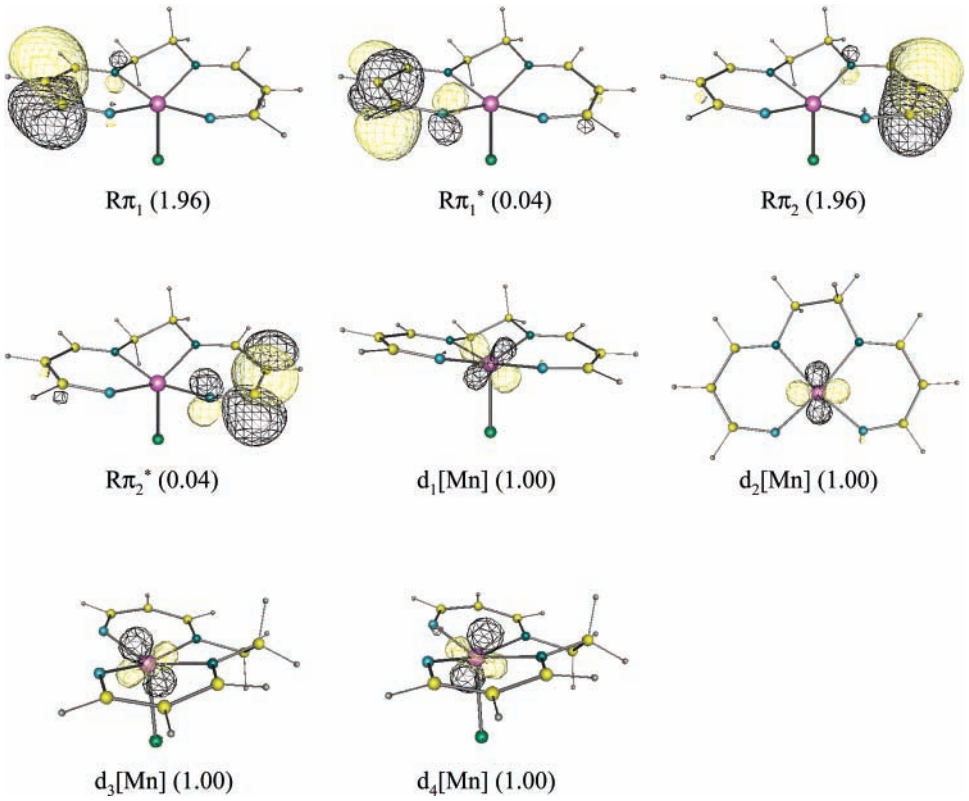


**Figure 6.** Mn(salen) CASSCF/6-31G* optimized geometry together with plots of the eight natural orbitals. Occupations are given below each illustration.

and triplet O products without the occurrence of spin flipping. Writing S[Mn(salen)] = 2 and S[O] = 1, we find that the possible spin states allowed for a combined species are S[oxo-(Mn(salen)] = 1, 2, 3. Hence the triplet and quintet oxoMn-(salen) species are permitted to dissociate to the high spin products, but the singlet species can dissociate only via spin flipping. No other theoretical work has discussed this point, which is salient to the chemistry of these catalytic compounds.

It is very likely that the recovery of dynamic correlation, i.e., MRMP2 type calculations, will stabilize the bound species relative to the dissociated products. However, the MRMP2 method is not size consistent and therefore calculations on the supersystem are required to obtain a comparable energy for the separated products. We have had problems converging CASSCF wave functions for this supersystem as changes in orbital orderings are observed. More specifically, an O[2p] orbital becomes slowly doubly occupied as the $O_{ax}$ atom is moved away from the Mn center, and therefore switches out of the active space and into the core orbital space. We are currently working to solve this problem to obtain energies for both the bound and dissociated systems which include a consistent recovery of the dynamic correlations.[24] At this stage we are unsure whether such energies will also predict spontaneous dissociation but we note that the oxo(salen)Mn species has not yet been conclusively isolated experimentally, and 30 kcal/mol is a sizable barrier to overcome for this system, even including higher levels of correlation.

**B. oxoMn(salen)$^-$.** The effect of adding an electron to the neutral oxoMn(salen) system was studied. Noting that CASSCF and MRMP2 predictions of energy splittings were in good agreement, only the CASSCF level of theory was used to study the oxoMn(salen)$^-$ anion.

*I. Doublet.* Geometry optimizations were started with initial active spaces and geometries corresponding to the singlet oxoMn(salen) species. The only difference being the inclusion of an extra active electron. This 10 orbital, 11 electron active space gave rise to 52 920 determinants with $M_s = {}^1/_2$. The optimized CASSCF/6-31G* geometry is shown in Figure 7, and absolute energies for both 6-31G* and ECP basis sets are given in Table 1. We see that the structure is relatively unchanged from the neutral singlet species except that the Mn−$O_{ax}$ and Mn−Cl distances have increased to 1.608 and 2.809 Å, respectively. The much larger Mn−Cl distance is most likely due to the presence of an extra electron in the vicinity of the Mn atom. The CASSCF/ECP optimized geometry is virtually indistinguishable from that obtained with the 6-31G* basis set. Predicted Mn−$O_{ax}$ and Mn−Cl distances are slightly different at 1.613 and 2.762 Å, respectively. NOs obtained with both basis sets very closely resembled those obtained for the singlet oxoMn(salen) species. CASSCF/6-31G* occupations of the R$\pi$1, R$\pi$1*, R$\pi$2, R$\pi$2*, $\sigma$(Mn$O_{ax}$), and $\sigma$*(Mn$O_{ax}$) orbitals are similar to all the systems described previously at 1.97, 0.03, 1.97, 0.03, 1.91, 0.09, respectively. Occupations for the remaining $\pi$1(Mn$O_{ax}$), $\pi$1*(Mn$O_{ax}$), $\pi$2(Mn$O_{ax}$), and $\pi$2*(Mn$O_{ax}$) orbitals are, as expected, different from previous systems at 1.81, 0.20, 1.95, and 1.04. These occupations indicate that the lowest energy doublet has its unpaired electron in the $\pi$1* orbital. Occupations of NOs obtained with the ECP basis set are virtually identical to those obtained with the 6-31G* basis set. Localizations of the core orbitals confirmed the existence of the d[$x^2-y^2$][Mn] lone pair seen in the neutral singlet. The electronic structure of the doublet oxoMn(salen)$^-$ species is illustrated in Figure 5.

*II. Quartet.* The active orbitals described above together with the localized d[$x^2-y^2$][Mn] orbital was used as a starting guess for calculations on the quartet oxoMn(salen) species. This 11 orbital, 13 electron active space contained 76 230 determinants with $M_s = {}^3/_2$. The optimized CASSCF/6-31G* geometry is

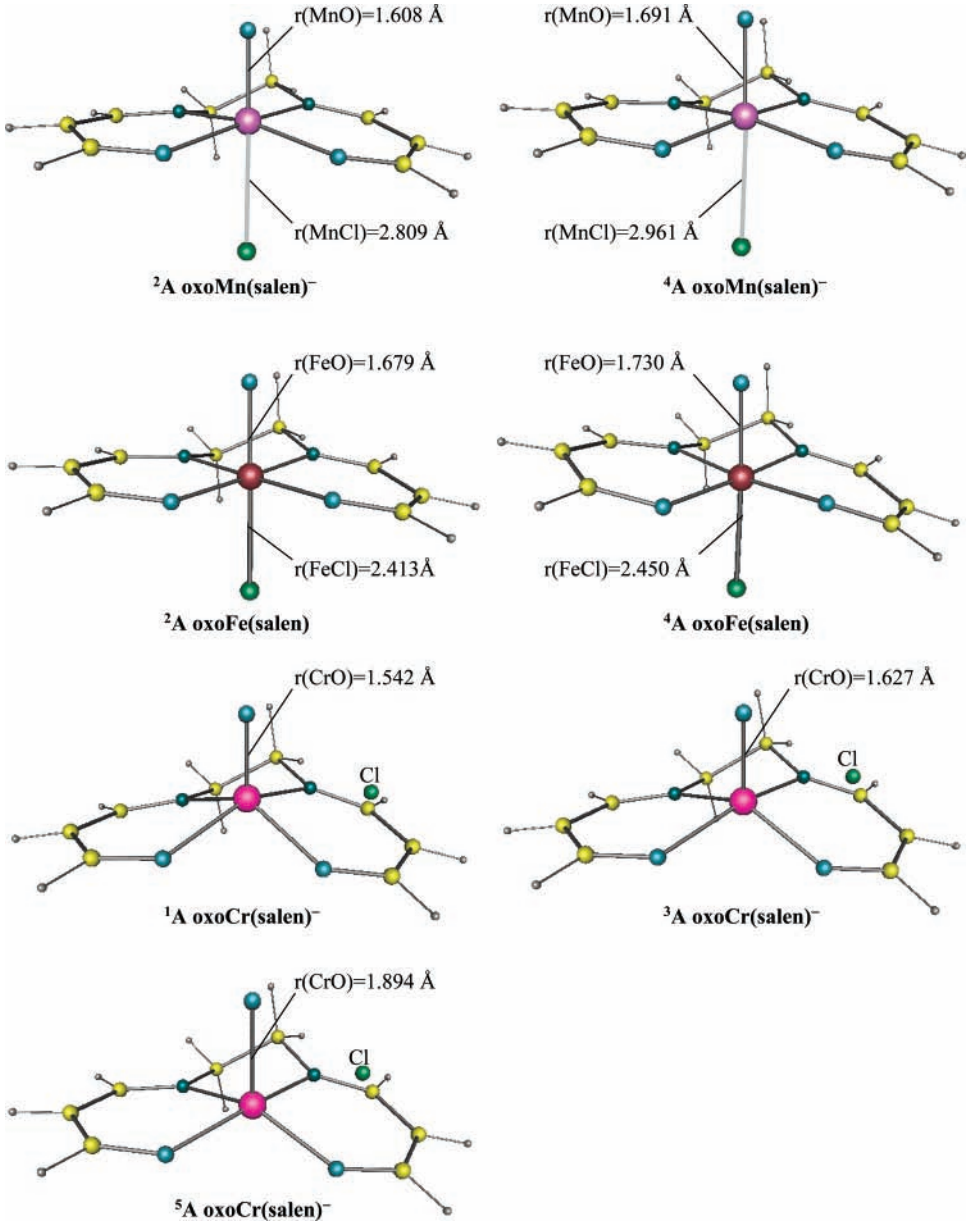


**Figure 7.** Illustration of optimized geometries of different electronic states of the oxoMn(salen)$^-$, oxoFe(salen), and oxoCr(salen)$^-$ species.

shown in Figure 7. We first observe that the quartet oxoMn-(salen)$^-$ species has a minimum and that Mn−$O_{ax}$ and Mn−Cl distances, at 1.691 and 2.961 Å, respectively, are longer than those in the doublet. The CASSCF/ECP geometry is essentially equivalent to that obtained using the 6-31G* basis. Predicted Mn−$O_{ax}$ and Mn−Cl distances are slightly different at 1.700 and 2.908 Å, respectively. NOs obtained with both basis sets are virtually identical to those seen in the triplet and quintet oxoMn(salen) systems. CASSCF/6-31G* occupations of the R$\pi$1, R$\pi$1*, R$\pi$2, and R$\pi$2* orbitals are virtually unchanged from previous systems at 1.97, 0.03, 1.96, and 0.04. The populations of the $\sigma$($MnO_{ax}$), and $\sigma$*($MnO_{ax}$) orbitals, at 1.78 and 0.22, indicate that correlation of the $\sigma$ bonding electrons is more important than in the other systems, a consequence of the larger Mn−$O_{ax}$ bond length. Occupations of the remaining $\pi$1-($MnO_{ax}$), $\pi$1*($MnO_{ax}$), $\pi$2($MnO_{ax}$), $\pi$2*($MnO_{ax}$), and d[$x^2-y^2$]-(Mn) orbitals are 1.94, 1.06, 1.94, 1.06, and 1.00, respectively, and these indicate that the quartet has the dominant $d^1\pi1^{*1}\pi2^{*1}$ configuration. Figure 5 illustrates the excitation from the doublet configuration, which gives rise to the quartet. CASSCF/ECP NO populations are identical to those given for the 6-31G* above. Absolute energies are given in Table 1 and energies relative to the doublet species are given in Table 2. We find that both 6-31G* and ECP basis sets predict the quartet to lie lower in energy than the doublet by 9 and 10 kcal/mol, respectively.

*III. Electron Affinity of the oxoMn(salen) Species.* From the absolute energies given in Table 1, we find that the CASSCF/6-31G* and CASSCF/ECP levels of theory predict electron affinities (EAs) of the singlet oxoMn(salen) complex to be −74 and −73 kcal/mol, respectively. The observation of a favorable EA for the oxoMn(salen) complex was not totally unexpected, but we did not expect such a large value. Calculations of EAs using basis sets without diffuse functions are likely to be underestimated or even the wrong sign if the electron attachment reaction is known to be favorable. We feel, therefore, that the oxoMn(salen) species is a very strong electrophile, and if anything, our prediction of the EA is underestimated. This finding is consistent with the reaction of this catalyst with the electron-rich double bond of olefins.

**C. oxoFe(salen).** For all previous systems, results using the 6-31G* and ECP basis sets at the CASSCF level of theory have

been in very good agreement. For this reason the oxoFe(salen) species was studied using only the 6-31G* basis set with identical active spaces to those described above for the oxoMn(salen)$^-$ species. Bound species were located for both doublet and quartet states. Their optimized geometries are illustrated in Figure 7. We find that the predicted Fe−$O_{ax}$ bond lengths are longer than their oxoMn(salen)$^-$ counterparts at 1.679 and 1.730 Å for the doublet and quartet states, respectively. Interatomic Fe−Cl distances for the doublet and quartet have decreased substantially to 2.413 and 2.450 Å, respectively, resembling those observed in the neutral oxoMn(salen) and Mn(salen) species. Absolute energies are given Table 1 and relative energies with respect to the doublet are given in Table 2. We find for the first time that the lower spin state is predicted to be slightly favored over the higher one, by a value of 3 kcal/mol. Such a small estimation of the energy difference means that we cannot say for sure which state is the lowest; however, we are quite certain that both are minima species. NOs for the doublet and quartet states were virtually indistinguishable from those seen in the respective related oxoMn(salen) species. Orbital occupations were slightly different from the oxoMn(salen)$^-$. Populations of the R$\pi$1, R$\pi$1*, R$\pi$2, R$\pi$2*, $\sigma$(Fe$O_{ax}$), $\sigma$*(Fe$O_{ax}$), $\pi$1(Fe$O_{ax}$), $\pi$1*(Fe$O_{ax}$), $\pi$2(Fe$O_{ax}$), and $\pi$2*(Fe$O_{ax}$) orbitals in the doublet were 1.97, 0.03, 1.96, 0.04, 1.82, 0.18, 1.58, 0.42, 1.92, and 1.08, respectively. These indicate that there are significant correlations into the $\sigma$*(Fe$O_{ax}$) and $\pi$1*(Fe$O_{ax}$) orbitals. As with the low spin oxoMn(salen) and oxoMn(salen)$^-$ species, localization of the core orbitals produced a d[$x^2-y^2$](Fe) lone pair. Occupations of the quartet R$\pi$1, R$\pi$1*, R$\pi$2, and R$\pi$2* orbitals were within 0.01 of those in the quartet oxoMn(salen)$^-$ species. Populations of the remaining $\sigma$(Fe$O_{ax}$), $\sigma$*(Fe$O_{ax}$), $\pi$1(Fe$O_{ax}$), $\pi$1*(Fe$O_{ax}$), $\pi$2(Fe$O_{ax}$), $\pi$2*(Fe$O_{ax}$), and d[$x^2-y^2$](Fe) orbitals were 1.80, 0.20, 1.87, 1.13, 1.85, 1.15, and 1.00, respectively. As for the doublet, there are nontrivial excitations into the Fe−$O_{ax}$ antibonding orbitals. These NO occupations indicate that the major configurations in the doublet and quartet species are equivalent to their respectively related oxoMn(salen)$^-$ species.

**D. oxoCr(salen)$^-$.** So far, at the CASSCF level of theory, the oxoMn(salen) complex is the only system for which spontaneous dissociation of the O atom is predicted upon electron excitation. Another system that demonstrates high enantioselectivities in epoxidations is the oxoCr(salen) complex.[26] A CASSCF study of this system is not straightforward due to the presence of empty d orbitals in excited states of this species and ground states of its related Cr(salen) complex. We are using other CI type methods to study these systems.[24] We can only say here that, similar to the oxoMn(salen) complex, higher spin states are the result of excitation of a d electron. However, the oxoCr(salen)$^-$ anion is isoelectronic to the oxoMn(salen) species and so studies on the nature of its electronic states were performed at the CASSCF/6-31G* level of theory. Identical active spaces to those described for the oxoMn(salen) species were used for the oxoCr(salen)$^-$ species. Optimized geometries are illustrated in Figure 7 and absolute energies are given in Table 1. In direct contrast with the oxoMn(salen) species, we found bound minima for all three singlet, triplet, and quintet states. In all three structures, the Cl atom has moved away from the central metal and prefers to reside on the edges of the ligand boundaries. Due to this Cl atom rearrangement, the singlet geometry is more pyramidal than the oxoMn(salen) structure and becomes gradually less so as the spin increases. Predicted Cr−$O_{ax}$ bond lengths, at 1.542, 1.627, and 1.894 Å for the singlet, triplet and quintet electronic states respectively, increase with spin. NOs share the same features as their oxoMn(salen) counterparts and occupations are reasonably similar. Relative energies of the singlet, triplet and quintet states are given in Table 2. We find, as for the oxoMn(salen) system, that the singlet and triplet states have very similar energies and the quintet state lies approximately 30 kcal/mol higher. An in depth discussion of the bonding in the oxoCr(salen)$^-$ species as well as its thermodynamic stability will be given elsewhere.[24]

## 4. Conclusions

Our CASSCF and MRMP2 calculations, using the 6-31G* and ECP basis sets, predict the singlet and triplet states to be very close in energy and the quintet to lie some 40 kcal/mol higher, at the singlet optimized geometries. These energy orderings are qualitatively consistent with the previous CCSD(T) calculations. However, geometry optimization of the triplet and quintet spin states at the CASSCF level of theory spontaneously dissociated the $O_{ax}$ atom, in sharp contrast to the oxoCr(salen)$^-$ system and previous DFT calculations but consistent with the highly reactive nature of the oxoMn(salen) species observed in experiment. On the basis of CASSCF calculations, we find that the lowest singlet electronic state of the oxo(salen)Mn species contains a triple Mn−$O_{ax}$ bond and a doubly occupied d[$x^2-y^2$](Mn) orbital. We also observe that the lowest triplet electronic state arises from a d[$x^2-y^2$](Mn) → $\pi$1*(Mn$O_{ax}$) transition and that the lowest quintet state is a result of a further $\pi$1(Mn$O_{ax}$) → $\pi$2*(Mn$O_{ax}$) electron excitation. We also find that an open shell SCF calculation for the triplet, starting from singlet optimized orbitals, gives a chemical description very different from that obtained at the CASSCF level of theory. This suggests that calculations based upon a single reference may not properly describe the system. This notion is supported by CASSCF calculations indicating, through analysis of NOs, that the system has multi-configurational character.

The separated products, $^5$A Mn(salen) + $^3$P O, are predicted to lie some 30 kcal/mol lower than the bound singlet oxo(salen)Mn species in the CASSCF calculations. This is the first calculation to determine this value and is important for understanding the thermochemistry of this catalyst as well as kinetic properties. Due to orbital reordering problems as the $O_{ax}$ atom is moved away from the Mn complex, MRMP2 energies for the dissociated super-system could not be obtained.

A study of the negative anion, oxo(salen)Mn$^-$, predicted bound doublet and quartet electronic states, with the doublet lying approximately 10 kcal/mol above the quartet ground state. From absolute energies an electron enthalpy (EA) of approximately −70 kcal/mol was obtained for the neutral oxoMn(salen) species, consistent with experimental evidence that the oxoMn(salen) species is a strong electrophile.

Investigation of the oxo(salen)Fe complex, isoelectronic with oxo(salen)Mn$^-$, also predicted bound doublet and quartet states with the quartet lying higher than the doublet by approximately 3 kcal/mol. The oxo(salen)Cr$^-$ species, which is isoelectronic with the oxo(salen)Mn complex, is predicted to have bound minima for the singlet, triplet, and quintet electronic states. These observations are in direct contrast to those seen for the oxoMn(salen) sytem. The oxo(salen)Cr$^-$ singlet and triplet species were predicted to be very close in energy and the quintet estimated to lie some 30 kcal/mol higher. These energy separations are similar to those observed for the oxoMn(salen) system.

The electronic structures for all species described above can be rationalized by the presence of a common set of orbitals.

Differences between electronic states arise directly from differing electron occupations of these orbitals, and this concept is illustrated in Figure 5.

This study presents results for the oxoX(salen) (X = Mn, $Mn^-$, $Cr^-$, Fe) systems that are consistent with the high reactivity and electrophilic nature of oxoMn(salen) as well as new insights into the possible reasons for the increased stability of Cr-substituted salen compounds. They also lead us to speculate that substitution of the metal can strongly affect the therapeutic properties of M(salen) compounds, especially in reactions with oxygen species similar to superoxide dismutase and catalase. Finally, the clear multiconfigurational nature of these compounds suggests that care must be taken in describing their electronic structure starting from single determinantal methods. Further studies will require higher levels of theory with more correlation to definitively determine the ground spin state of the oxoMn(salen) species.

**Acknowledgment.** We thank Dr. Yuri G. Abashkin and Dr. Igor Topol for helpful discussions. This project has been funded in whole or in part with Federal funds from the National Cancer Institute, National Institutes of Health, under Contract No. N01-CO-12400. The content of this publication does not necessarily reflect the views of policies of the Department of Health and Human Services, nor does mention of trade names, commercial products, or organization imply endorsement by the U.S. Government.

**Supporting Information Available:** All CASSCF optimized geometries are given in the Supporting Information. This material is available free of charge via the Internet at http://pubs.acs.org.

## References and Notes

(1) (a) In *Comprehensive Organometallic Chemistry II*; Wilkinson, G., Stone, F. G. A., Abel, E. W., Hegedus, L. S., Eds.; Pergamon: New York, 1995; Vol. 12, Chapter 11.1, pp 159−202. (b) Katsuki, T. *Coord. Chem. Rev.* **1995**, *140*, 189.

(2) (a) Jacobsen, E. N. In *Catalytic Asymmetric Synthesis*; Ojima, I., Ed.; VCH: New York, 1993; p 159. (b) Jacobsen, E. N.; Finney, N. S. *Chem. Biol.* **1994**, *1*, 85. (c) Katsuki, T. *J. Mol. Catal. A: Chem.* **1996**, *113*, 87. (d) Dalton, C. T.; Ryan, K. M.; Wall, V. M.; Bousquet, C.; Gilheany, D. G. *Top. Catal.* **1998**, *5*, 75.

(3) Fu, H.; Look, G. C.; Zhang, W.; Jacobsen, E. N.; Wong, C.-H. *J. Org. Chem.* **1991**, *56*, 6497.

(4) (a) Srinivasan, K.; Michaud, P.; Kochi, J. K. *J. Am. Chem. Soc.* **1986**, *108*, 2309. (b) Finney, N. S.; Pospisil, P. J.; Chang, S.; Palucki, M.; Konsler, R. G.; Hansen, K. B.; Jacobsen, E. N. *Angew. Chem., Int. Ed. Engl.* **1997**, *36*, 1720. (c) Linker, T. *Angew. Chem., Int. Ed. Engl.* **1997**, *36*, 2060.

(5) (a) Norrby, P.-O.; Linde, C.; Akermark, B. *J. Am. Chem. Soc.* **1995**, *117*, 11035. (b) Hamada, T.; Fukuda, T.; Imanishi, H.; Katsuki, T. *Tetrahedron* **1996**, *52*, 515. (c) Linde, C.; Arnold, M.; Norrby, P.-O.; Akermark, B. *Angew. Chem., Int. Ed. Engl.* **1997**, *36*, 1723.

(6) Palucki, M.; Finney, N. S.; Pospisil, P. J.; Guler, M. L.; Ishida, T.; Jacobsen, E. N. *J. Am. Chem. Soc.* **1998**, *120*, 948 and references therein.

(7) Doctrow, S. R.; Hoffman, K.; Marcus, C. B.; Musleh, W.; Bruce, A.; Baudry, M.; Malfroy, B. *Adv. Pharmacol.* **1997**, *38*, 247.

(8) Linde, C.; Akermark, B.; Norrby, P.-O.; Svensson, M. *J. Am. Chem. Soc.* **1999**, *121*, 5083.

(9) (a) Cavallo, L.; Jacobsen, H. *Angew. Chem., Int. Ed. Engl.* **2000**, *39*, 589. (b) Strassner, T.; Houk, K. N. *Org. Lett.* **1999, *1***, 419.

(10) Abashkin, Y. G.; Collins, J. R.; Burt, S. K. *Inorg. Chem.* **2001**, *40*, 4040.

(11) The name of the neutral model compound is chloro-4,4′-(1,2-ethanediyldinitrilo)bis(2-pentanonato)((2−)-*N*,*N*′,*O*,*O*′)-*m*-oxomanganese.

(12) (a) Ditchfield, R.; Hehre, W. J.; Pople, J. A. *J. Chem. Phys.* **1971**, *54*, 724. (b) Hehre, W. J.; Ditchfield, R.; Pople, J. A. *J. Chem. Phys.* **1972**, *56*, 2257. (c) Hariharan, P. C.; Pople, J. A. *Theor. Chim. Acta* **1973**, *28*, 213. (d) Francl, M. M.; Pietro, W. J.; Hehre, W. J.; Binkley, J. S.; Gordon, M. S.; DeFrees, D. J.; Pople, J. A. *J. Chem. Phys.* **1982**, *77*, 3654. (e) Rassolov, V. A.; Pople, J. A.; Ratner, M. A.; Windus, T. L. *Chem. Phys.* **1998**, *109*, 1223.

(13) (a) Stevens, W. J.; Basch, H.; Krauss, M. *J. Chem. Phys.* **1984**, *81*, 6026. (b) Stevens, W. J.; Krauss, M.; Basch, H.; Jasien, P. G. *Can. J. Chem.* **1992**, *70*, 612.

(14) Schmidt, M. W.; Baldridge, K. K.; Boatz, J. A.; Elbert, S. T.; Gordon, M. S.; Jensen, J. H.; Koseki, S.; Matsunaga, N.; Nguyen, K. A.; Su, S. J.; Windus, T. L.; Dupuis, M.; Montgomery, J. A. *J. Comput. Chem.* **1993**, *14*, 1347. www.msg.ameslab.gov/GAMESS/GAMESS.html

(15) Ivanic, J.; Ruedenberg, K. *Theor. Chem. Acc.* **2001**, *106*, 339.

(16) Chaban, G.; Schmidt, M. W.; Gordon, M. S. *Theor. Chem. Acc.* **1997**, *97*, 88.

(17) This code is based upon the ideas presented in the papers: (a) General second-order MCSCF theory: A Density Matrix Directed Algorithm. Lengsfield, B. H., III. *J. Chem. Phys.* **1980**, *73*, 382. (b) The use of the Augmented Matrix in MCSCF Theory. Yarkony D. R. *Chem. Phys. Lett.* **1981**, *77*, 634.

(18) Fletcher, G. To be published.

(19) (a) Hirao, K. *Chem. Phys. Lett.* **1992**, *190*, 374. (b) Hirao, K. *Chem. Phys. Lett.* **1992**, *196*, 397. (c) Hirao, K. *Int. J. Quantum Chem.* **1992**, *S26*, 517. (d) Hirao, K. *Chem. Phys. Lett.* **1993**, *201*, 59.

(20) (a) Nakano, H. *J. Chem. Phys.* **1993**, *99*, 7983. (b) Nakano, H. *Chem. Phys. Lett.* **1993**, *207*, 372. (c) Nakano, H.; Nakayama, K.; Hirao, K.; Dupuis, M. *J. Chem. Phys.* **1997**, *106*, 4912. (d) Hashimoto, T.; Nakano, H.; Hirao, K. *J. Mol. Struct. (THEOCHEM)* **1998**, *451*, 25.

(21) Edmiston, C.; Ruedenberg, K. *Rev. Mod. Phys.* **1963**, *35*, 457.

(22) Olson, R. M.; Bode, B.; Gordon, M. S. *WinMolPlt, A Computational Chemistry Graphical Interface.*

(23) Bauschlicher, C. W., Jr. *J. Chem. Phys.* **1980**, *72*, 880.

(24) Ivanic, J.; Collins, J. R.; Burt, S. K. Work in progress.

(25) Pospisil, P. J.; Carsten, D. H.; Jacobsen, E. N. *Chem. Eur. J.* **1996**, *2*, 974.

(26) (a) Bousquet, C.; Gilheany, D. G. *Tetrahedron Lett.* **1995**, *36*, 7739. (b) Ryan, K. M.; Bousquet, C.; Gilheany, D. G. *Tetrahedron Lett.* **1999**, *40*, 3613. (c) Daly, A. M.; Dalton, C. T.; Renehan, M. F.; Gilheany, D. G. *Tetrahedron Lett.* **1999**, *40*, 3617. (d) Daly, A. M.; Renehan, M. F.; Gilheany, D. G. *Org. Lett.* **2001**, *3*, 663. (e) O'Mahony, C. P.; McGarrigle, E. M.; Renehan, M. F.; Ryan, K. M.; Kerrigan, N. J.; Bousquet, C.; Gilheany, D. G. *Org. Lett.* **2001**, *3*, 3435.